

Magnetic silica nanoparticle-supported copper complex as an efficient catalyst for the synthesis of novel triazolopyrazinylacetamides with improved antibacterial activity

Mohammad Sadegh Asgari^{1,3}, Saghi Sepehri², Saeed Bahadorikhalili¹, Parviz Rashidi Ranjbar¹, Rahmatollah Rahimi³, Ahmad Gholami⁴, Aboozar Kazemi^{4,5}, Mehdi Khoshneviszadeh⁴, Bagher Larijani⁶, Mohammad Mahdavi^{6*}

¹ School of Chemistry, College of Science, University of Tehran, P. O. Box 14155-6455, Tehran, Iran

² Department of Medicinal Chemistry, School of Pharmacy, Ardabil University of Medical Sciences, Ardabil, 5618953141, Iran

³ Department of Chemistry, Iran University of Science and Technology, Narmak, Tehran 16846-13114, Iran; e-mail: sadegh.asgari.1@gmail.com

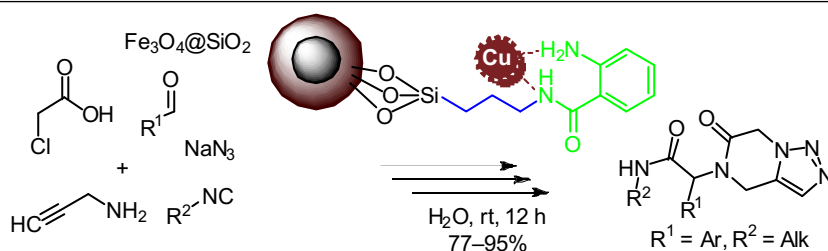
⁴ Pharmaceutical Science Research Center, Shiraz University of Medical Sciences, Shiraz, Iran

⁵ Department of Pharmaceutical Biotechnology, School of Pharmacy, Shiraz University of Medical Sciences, Shiraz, Iran

⁶ Endocrinology and Metabolism Research Center, Endocrinology and Metabolism Research Institute, Tehran University of Medical Sciences, Tehran, Iran; e-mail: momahdavi@sina.tums.ac.ir

Published in Khimiya Geterotsiklicheskikh Soedinenii, 2020, 56(4), 488–494

Submitted September 29, 2019
Accepted after revision January 21, 2020



A novel superparamagnetic iron oxide modified with copper via 2-aminobenzamide is synthesized by the modification of $\text{Fe}_3\text{O}_4@\text{SiO}_2$ with amine, followed by the reaction with isatoic anhydride. The catalyst is fully characterized by various methods. The catalytic activity of the catalyst is evaluated in the synthesis of a series of novel *N*-alkyl-2-aryl-2-(6-oxo-6,7-dihydro[1,2,3]triazolo[1,5-*a*]pyrazin-5(4*H*)-yl)acetamide analogs. Antibacterial activity of the synthesized compounds is evaluated. The catalyst is recoverable and shows excellent reusability in 10 sequential runs.

Keywords: nanoparticle-supported copper catalyst, triazole, antibacterial agents, click reaction, structure–activity relationship.

About half of all deaths in tropical countries are caused by infectious diseases. Although the number of deaths from bacterial infections has decreased in the developed countries, these infections remain a problem in undeveloped regions. Antibiotics are effective weapons to fight against bacterial infections, but their overuse has put pressure on bacteria to develop resistance.¹ The global spread of antibiotic-resistant infections is a serious problem which threatens global healthcare.² The discovery and development of antibiotics has been vital to human

survival, and has added an average of 20 years to the human lifetime.³ Gram-negative and Gram-positive pathogens are responsible for the majority of hospital-acquired and community-acquired infections, resulting in wide mortality and burden on worldwide healthcare system.⁴ One of the attractive scaffolds for researchers in making new therapeutic agents is triazole structure. This nitrogen-containing heterocycle is prominent among pharmaceuticals approved by FDA.⁵ 1,2,3-Triazole ring is attractive connecting unit, since it is stable to metabolic

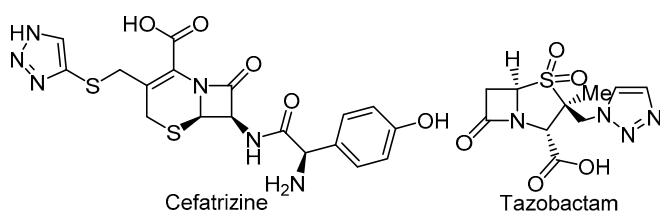


Figure 1. Chemical structures of commercial triazole-containing antibacterial drugs cefatrizine and tazobactam.

degradation, oxidative/reductive conditions and actively participates in binding to biomolecular targets and improves solubility of the molecule by hydrogen bonding and dipole interactions.⁶ 1,2,3-Triazoles are extensively used in medicinal chemistry because of their easy synthesis through click reaction and attractive features.⁷ 1,2,3-Triazole and its derivatives have attracted a great deal of interest due to their varied biological activities such as antifungal,⁸ antibacterial,⁹ antitubercular,¹⁰ anticancer,¹¹ and antiviral.¹² This heterocyclic moiety has gained special attention in the discovery of new antibiotics because numerous drug compounds containing 1,2,3-triazole group, such as for example cefatrizine and tazobactam, are used for the treatment of bacterial infections (Fig. 1).

Click chemistry is a good synthetic method applying several near-perfect chemical transformations for the synthesis and assembly of chemical scaffolds with potential biological activity.¹³ These reactions are modular, extensive in scope, give very high yields, they are stereospecific and generate only harmless byproducts that can be removed by nonchromatographic techniques.¹³ The click chemistry concept has received a considerable use in many fields of chemical science, including drug design and chemical investigations for the discovery of biologically active compounds.^{6,14} In addition, Ugi/alkyne-azide cycloaddition reaction is applied for the synthesis of fused triazolo derivatives.¹⁵

The application of copper in catalytic processes has attracted great attention in the last decade. The different oxidation states of copper associates well with a large number of different functional groups *via* Lewis acid interactions or π -coordination. These features confer a remarkably broad range of activities allowing copper to catalyze the oxidation, as well as click reactions.^{15,16} In recent years, Cu-promoted processes have evolved into viable alternatives to the more widely practiced Pd-catalyzed reactions.¹⁷ The Cu-based methods are distinguished by their broad scope, high efficiency, and mild reaction conditions, thus making them attractive vehicles for further applications. Although the synthesis and catalytic activities of copper catalysts have been successfully demonstrated, their separation from the reaction mixture and recycling are tedious, which limits their use for practical applications. Therefore, to overcome mentioned difficulties, heterogenized copper catalysts on solid supports has received increased attention. By immobilizing homogeneous catalysts on insoluble supports, the advantages of both homogeneous as well as heterogeneous catalysts are achieved, so that without losing catalytic activity the catalysts can be separated easily from the desired products by a simple filtration. During the past years, several solid supports have been efficiently prepared.^{18,19} Immobilized copper catalysts on solid supports have been applied in several organic

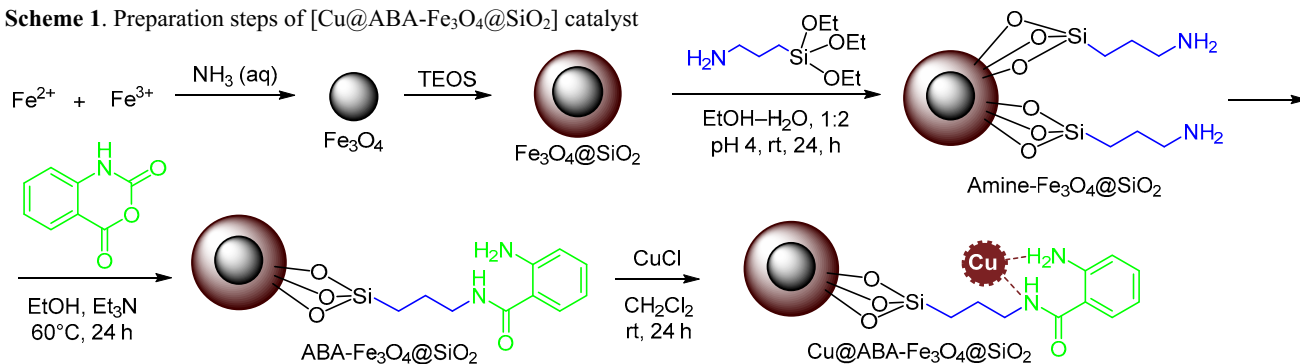
transformations, for example, oxygenation at benzylic positions,²⁰ alkane oxidation,²¹ alcohol oxidation,²² click reactions,²³ reductive coupling reactions.²⁴ The catalytic reduction of nitro group is probably one of the emerging areas in catalytic organic chemistry that might have a tremendous impact in chemical industry in the next decades.

Among the wide range of solid supports for transition metal catalysts, magnetic nanoparticles have displayed high applicability and are known as effective research tools to improve novel and operative recoverable catalysts. Magnetically separable systems have attracted a great deal of attention as an interesting alternative to improve the efficient separation of heterogeneous catalysts using an external magnet thus providing improved reusability.²⁵ Their widespread usage and versatility make magnetic silica core-shell nanoparticles excellent and interesting supporting materials for providing new and improved green catalysts. Magnetic nanoparticles can offer very promising features as catalyst supports due to their large specific surface areas and magnetic properties, which facilitate the separation of the catalyst upon reaction completion.²⁶

Although magnetic silica core-shell nanoparticles, thanks to the nanometric sizes, are well dispersed in many solvents, they cannot provide a suitable exposure of their catalytically active centers in the proximity of organic substrates, especially when hydrophilic solvents are used as the reaction medium. Therefore, we were interested in designing and preparing a novel catalyst system by emphasizing controlling its high dispersion in hydrophilic environment-friendly ethylene glycol while avoiding time-consuming recycling stages. Following our previous efforts on extending nanoparticles as supports for homogeneous transition metal catalysts on one hand, and synthesis of novel biologically active compounds on the other hand, hereby we report a copper-2-aminobenzamide (ABA) complex covalently attached to modified magnetic silica core-shell nanoparticles as an efficient catalyst for the synthesis of a series of *N*-alkyl-2-aryl-2-(6-oxo-6,7-dihydro-[1,2,3]triazolo[1,5-*a*]pyrazin-5(4*H*)-yl)acetamide derivatives. The synthesized compounds have also been screened for their antibacterial activity *in vitro*. Various functional groups were introduced into the target compounds in order to investigate preliminary structure–activity relationship.

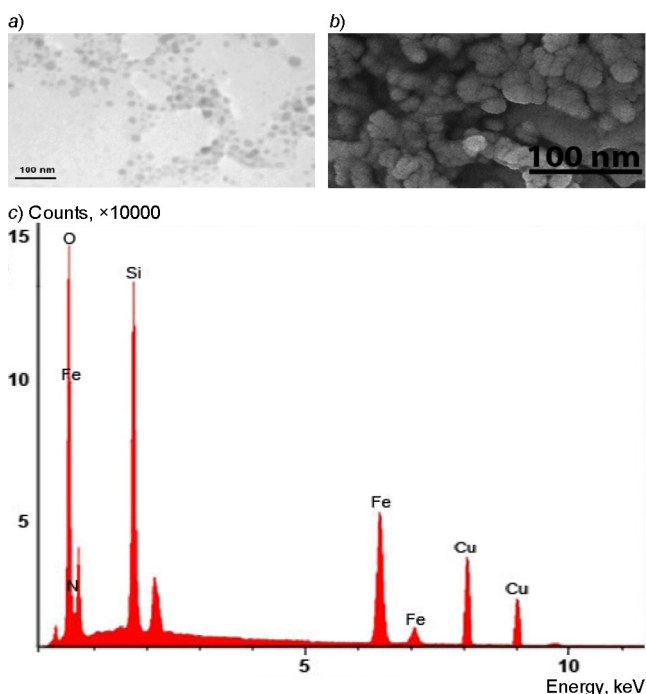
[Cu@ABA-Fe₃O₄@SiO₂] catalyst was synthesized by the immobilization of copper on the surface of the modified magnetic iron oxide nanoparticles. Superparamagnetic iron oxide nanoparticles were prepared by the coprecipitation of Fe²⁺ and Fe³⁺ in basic media. The superparamagnetic iron oxide nanoparticles were then encapsulated by silica, followed by the reaction with 3-aminopropyltriethoxysilane to introduce active amine groups on the surface of the nanoparticles. The [Amine-Fe₃O₄@SiO₂] finally reacted with 2*H*-3,1-benzoxazine-2,4(1*H*)-dione to form amino-benzamide-modified magnetic nanoparticles. This structure was used as a copper support to form [Cu@ABA-Fe₃O₄@SiO₂] catalyst. The step by step preparation of the catalyst is presented in Scheme 1.

The exact structure of [Cu@ABA-Fe₃O₄@SiO₂] catalyst was studied by several methods including field emission scanning electron microscopy (FE-SEM), transmission electron microscopy (TEM), inductively coupled plasma

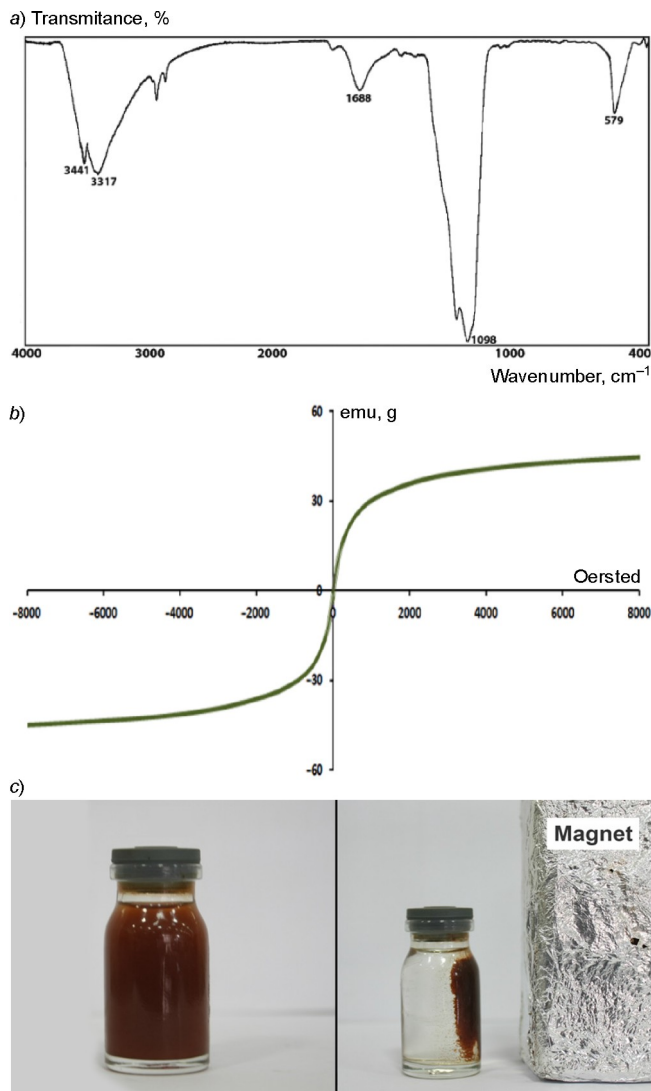
Scheme 1. Preparation steps of [Cu@ABA-Fe₃O₄@SiO₂] catalyst

atom emission spectroscopy (ICP-AES), and Fourier transform infrared spectrometry (FT-IR). Electron microscope images, including FE-SEM and TEM are presented in Figure 2. FE-SEM results (Fig. 2a) show the morphology of the catalyst to be spherical with the average particle size of about 25 nm. The TEM image, presented in Figure 2b, confirms the structure and the particle sizes of the catalyst. Figure 2c shows the energy-dispersive X-ray spectroscopy (EDS) analysis of [Cu@ABA-Fe₃O₄@SiO₂] catalyst. It could be seen that all the expected elements, including Fe, Si, O, C, and N could be seen in EDS spectrum. In addition, copper is also seen in EDS spectrum, which confirm the presence of Cu in the structure of [Cu@ABA-Fe₃O₄@SiO₂] catalyst.

To prove the structure of the synthesized catalyst, FT-IR spectroscopy was applied (Fig. 3a). The FT-IR spectrum of the catalyst shows an absorption at 579 cm⁻¹, which represents Fe–O vibrations. Si–O vibrations show an intense peak at 1098 cm⁻¹. In addition, the band at 1688 cm⁻¹ can be assigned to the carbonyl group in the structure of the catalyst. Vibration bands at 3441 and 3317 cm⁻¹ can be assigned to O–H and N–H vibrations, respectively.

**Figure 2.** a) FE-SEM image, b) TEM image, and c) EDS results of [Cu@ABA-Fe₃O₄@SiO₂] catalyst.

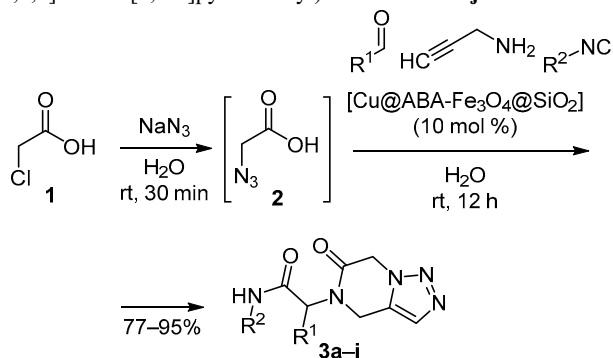
The magnetic behavior of the catalyst was studied by vibrating-sample magnetometer (VSM) method. The VSM curve is presented in Figure 3b. The magnetic hysteresis measurement was done using VSM in an applied magnetic field at room temperature with the field sweeping from –8000 to +8000 Oe to assay the magnetic behavior of catalyst. The S-type magnetization hysteresis loop confirmed the superparamagnetic nature of [Cu@ABA-Fe₃O₄@SiO₂] catalyst. For the sake of better magnetic behavior demonstra-

**Figure 3.** a) FT-IR spectrum, b) VSM curve, and c) magnetic separation of [Cu@ABA-Fe₃O₄@SiO₂] catalyst.

tion of the catalyst, the separation of [Cu@ABA-Fe₃O₄@SiO₂] by an external magnet is presented in Figure 3c. Moreover, the copper content of the catalyst was determined to be 2 mmol per gram of the catalyst.

The synthetic route for the newly synthesized compounds is outlined in Scheme 2. This reaction was performed at room temperature in H₂O. Sodium azide was added to 2-chloroacetic acid (**1**) at room temperature in H₂O to yield azide **2**. Then, without isolation of azide **2**, aromatic aldehyde, prop-2-yn-1-amine, alkyl isocyanide, and catalytic amount of [Cu@ABA-Fe₃O₄@SiO₂] catalyst were added to the reaction mixture to give the desired products **3a–j**. (Scheme 2). Chemical structures of the synthesized compounds were confirmed by ¹H and ¹³C NMR, FT-IR spectroscopy, and elemental analysis.

Scheme 2. Synthesis of *N*-alkyl-2-aryl-2-(6-oxo-6,7-dihydro-4*H*-[1,2,3]triazolo[1,5-*a*]pyrazin-5-yl)acetamides **3a–j**



Antibacterial activity of all synthesized compounds was screened against Gram-negative and Gram-positive bacterial strains including *Escherichia coli*, *Staphylococcus aureus*, *Pseudomonas aeruginosa*, *Enterococcus faecalis*. Ampicillin was tested under the same conditions as the reference drug. The results expressed as minimum inhibitory concentrations (MICs, µg/ml) are summarized in Table 1. Compound **3a** showed the most potent antibacterial activity against *E. coli* and *E. faecalis* strains (10.31 and 20.62 µg/ml, respectively). But compounds **3g** and **3h** were most effective against both *S. aureus* and *P. aeruginosa* strains, with MIC value of 82.5 µg/ml. It is noteworthy that compounds **3a** and **3f** both have MIC values 20.62 µg/ml against *E. coli* but 10.31 and 20.62 µg/ml against *E. faecalis*, respectively. This indicates that their efficacy is comparable to clinical antibiotics such as ampicillin (15.60 µg/ml against *E. coli* and 6.26 µg/ml against *E. faecalis*).

However, all compounds exhibited weak to good inhibitory effect against the growth of all strains. This may be attributed to the poor ability of these compounds to penetrate the outer membrane of bacteria. Compound **3g** having monomethoxyphenyl group and compound **3h** with trimethoxyphenyl group exhibited similar levels of *in vitro* antibacterial activity, while compound **3e** bearing 4-chlorophenyl group, displayed weaker *in vitro* antibacterial activity compared to compounds **3g** and **3h** against *S. aureus* and *P. aeruginosa* strains. In general, compounds bearing cyclohexane moiety at the NH amide position showed superior activity against all tested bacteria than

Table 1. Antibacterial activity of the synthesized compounds **3a–j** (minimal inhibition concentration (MIC), µg/ml)

Compound	R ¹	R ²	<i>E. coli</i>	<i>S. aureus</i>	<i>P. aeruginosa</i>	<i>E. faecalis</i>
3a			20.62	165	165	10.31
3b			165	82.5	165	20.62
3c			41.25	82.5	165	20.62
3d			41.25	165	82.5	165
3e			20.62	165	165	82.5
3f			20.62	82.5	165	20.62
3g			20.62	82.5	82.5	82.5
3h			20.62	82.5	82.5	82.5
3i			41.25	165	82.5	82.5
3j			41.25	165	82.5	82.5
Ampicillin	–	–	15.60	13.12	15.60	6.25

compounds bearing *tert*-butyl moiety at the same position (e. g., compounds **3a** and **3c** vs compounds **3e** and **3h**).

Compounds with electron-withdrawing substituents in the phenyl ring, such as chlorine (compound **3c**) exhibited more potent activity with MICs 20.62 and 82.5 µg/ml against *E. faecalis* and *S. aureus*, while compounds with electron-donating substituents such as methoxy (compound **3g**), methyl (compound **3d**), and isopropyl (compound **3i**) groups in the *para* position of phenyl ring with MICs 82.5 and 165 µg/ml showed weak to moderate activity. In addition, obviously that methyl substitution at the *para* position of phenyl ring (compound **3d**) decreased the inhibitory effects compared to the corresponding compound **3j** substituted at *meta* position against three strains of *E. coli*, *S. aureus*, and *E. faecalis*. Methyl functionality

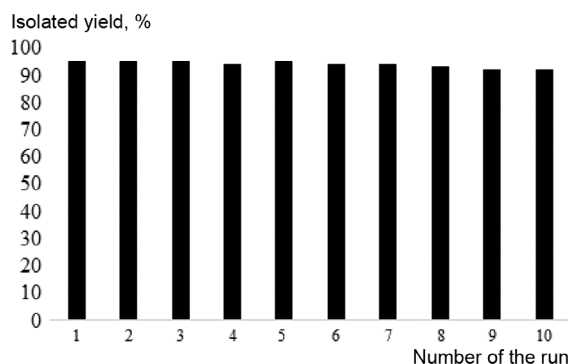


Figure 4. Recovery results of [Cu@ABA-Fe₃O₄@SiO₂] catalyst in 10 sequential reactions of the compound **3a** synthesis.

in *ortho* position showed to be much more active against the studied bacteria than that in *para* position (Table 1).

Compounds **3i,j** both with isopropyl group in the *para* position of phenyl ring and with either cyclohexane at NH amide position (compound **3i**) or *tert*-butyl group at NH amide position (compound **3j**) exhibited similar levels of *in vitro* antibacterial activity against four strains.

An important feature of [Cu@ABA-Fe₃O₄@SiO₂] catalyst is its reusability. For the reusability study, the catalyst was isolated after the reaction completion, washed, and used in the next reaction. This study was performed for 10 sequential runs. The recovery results are presented in Figure 4. It can be observed that, the desired products are obtained in high isolated yields even after 10 runs, without essential decrease in the catalyst activity. For the stability studying, the catalyst was stirred in the reaction conditions for 24 h. The catalyst was separated using a magnet and the solution was analyzed by ICP method. The result showed that the copper content in the solution was less than 1 ppm, which proves the stability of the catalyst in the reaction conditions.

In this research, a novel catalyst based on the immobilization of copper onto modified superparamagnetic iron oxide *via* aminobenzamide is introduced. The catalyst is synthesized by the modification of Fe₃O₄@SiO₂ with propylamine, followed by the reaction with 2*H*-3,1-benzoxazine-2,4(1*H*)-dione. The successful formation of the catalyst was proved by various characterization methods. Catalyst proved to be recoverable and demonstrated excellent reusability in 10 sequential runs. The catalytic activity of the catalyst was evaluated in the synthesis of novel *N*-alkyl-2-aryl-2-(6-oxo-6,7-dihydro-4*H*-[1,2,3]triazolo[1,5-*a*]pyrazin-5-yl)acetamides. Several products, bearing wide range of functional groups were synthesized. The antibacterial activity of the synthesized compounds was evaluated against *E. coli*, *S. aureus*, *P. aeruginosa*, and *E. faecalis*, and the results showed good activity of the compounds against the tested bacteria.

Experimental

IR spectra were recorded on a Shimadzu FT-IR 550 spectrometer in KBr pellets. ¹H and ¹³C NMR spectra were recorded on a Bruker Avance spectrometer (500 and 125 MHz, respectively) in DMSO-*d*₆ solution with TMS as internal standard. Elemental analysis was performed on a VarioEL system in CHNS mode. ICP analysis was performed using an inductively coupled plasma (ICP) analyzer (Varian,

Vista-Pro). Transmission electron microscopy (TEM) analyses were performed on a Philips model CM 10 instrument. Energy-dispersive X-ray spectroscopy analyses for the characterization of the catalyst were recorded on a GNR Explorer machine. Melting points were determined in open capillary tubes on a Barnstead Electrothermal 9100 BZ circulating oil melting point apparatus. The reaction monitoring was accomplished by TLC on silica gel PolyGram SILG/UV254 plates. Column chromatography was carried out on columns of silica gel 60 (70–230 mesh). Chemicals were purchased from Merck, Acros, and Aldrich chemical companies and used without further purification.

Preparation of [Amine-Fe₃O₄@SiO₂]. A solution of 3-aminopropyltriethoxysilane (0.1 g, 0.45 mmol) in EtOH (30 ml) was added dropwise to a vigorously stirring mixture of Fe₃O₄@SiO₂ nanoparticles (100 mg), prepared according to the reported procedure,¹⁹ in EtOH–H₂O, 1:2 (30 ml) and HCl (pH 4). After vigorous stirring for 24 h, the solution was filtered off and washed thoroughly. The residue was dried at 100°C under reduced pressure for 12 h.

Preparation of [ABA-Fe₃O₄@SiO₂]. 2*H*-3,1-Benzoxazine-2,4(1*H*)-dione (450 mg, 2.76 mmol) was added to a mixture of [Amine-Fe₃O₄@SiO₂] (100 mg) and Et₃N (0.1 g, 1.7 mmol) in EtOH and stirred at 60°C for 24 h. Afterward, the solid was separated by an external magnet, washed with EtOH (3×10 ml), and dried under reduced pressure at 60°C.

Preparation of [Cu@ABA-Fe₃O₄@SiO₂]. CuCl (495 mg, 5 mmol) was added to a mixture of [ABA-Fe₃O₄@SiO₂] (0.1 g) in dry CH₂Cl₂ (50 ml) and stirred at room temperature under argon atmosphere for 24 h. The obtained solid was magnetically separated and washed with CH₂Cl₂ (2×10 ml) and Et₂O (2×10 ml). [Cu@ABA-Fe₃O₄@SiO₂] catalyst was obtained after drying under reduced pressure for 12 h.

Synthesis of *N*-alkyl-2-aryl-2-(6-oxo-6,7-dihydro-4*H*-[1,2,3]triazolo[1,5-*a*]pyrazin-5-yl)acetamides **3a–j** (General method). 2-Chloroacetic acid (**1**) (1 mmol) and NaN₃ (1 mmol) were added into a round-bottom flask containing H₂O (5 ml) and stirred for 30 min at room temperature. Then aromatic aldehyde (2 mmol), prop-2-yn-1-amine (1 mmol), alkyl isocyanide (1 mmol), and [Cu@ABA-Fe₃O₄@SiO₂] (10 mol %) were added, and the reaction mixture was stirred at room temperature for 12 h. After the completion of the reaction, the catalyst was separated by an external magnet. H₂O was added to the reaction mixture, the resulting precipitate was filtered off.

For studying the reusability of [Cu@ABA-Fe₃O₄@SiO₂] catalyst, the reaction of 2-chloroacetic acid, 3,4,5-trimethoxybenzaldehyde, propargylamine, and cyclohexyl isocyanide was selected as the model reaction. The reaction was performed according to the conditions, mentioned above. After the completion of the reaction, the catalyst was separated from the reaction mixture, using an external magnet and was used directly in the next reaction. The reusability study was evaluated for 10 sequential runs. Results are presented in Figure 4.

***N*-Cyclohexyl-2-(6-oxo-6,7-dihydro[1,2,3]triazolo[1,5-*a*]pyrazin-5(4*H*)-yl)-2-(3,4,5-trimethoxyphenyl)acetamide (**3a**).** Yield 0.420 g (95%), white solid, mp 220–222°C. IR spectrum, ν , cm⁻¹: 3120, 1661, 1625, 1434, 1065. ¹H NMR spectrum, δ , ppm (*J*, Hz): 8.32 (1*H*, d, *J* = 7.8, NH); 7.63 (1*H*, s, H triazole); 6.54 (2*H*, s, H Ar); 6.20 (1*H*, s,

CH); 5.21 (2H, dd, $J = 17.4$, $J = 17.4$, CH₂); 4.91 (1H, d, $J = 16.1$, CH₂ pyrazine); 4.13 (1H, d, $J = 16.2$, CH₂ pyrazine); 3.74 (6H, s, 2OCH₃); 3.67–3.57 (7H, m, OCH₃, CH cyclohexyl); 1.84–1.53 (5H, m, CH₂ cyclohexyl); 1.28–1.10 (5H, m, CH₂ cyclohexyl). ¹³C NMR spectrum, δ , ppm: 167.9; 163.6; 153.5; 137.8; 130.5; 129.6; 129.5; 106.7; 60.5; 59.4; 56.4; 49.2; 48.2; 32.7; 32.4; 25.6; 24.9. Found, %: C 59.57; H 6.64; N 15.77. C₂₂H₂₉N₅O₅. Calculated, %: C 59.58; H 6.59; N 15.79.

***N*-tert-Butyl-2-(2-methylphenyl)-2-(6-oxo-6,7-dihydro-[1,2,3]triazolo[1,5-*a*]pyrazin-5(4*H*)-yl)acetamide (3b).** Yield 0.330 g (97%), white solid, mp 235–237°C. IR spectrum, ν , cm⁻¹: 3122, 1661, 1617, 1429, 1061. ¹H NMR spectrum, δ , ppm (J , Hz): 8.06 (1H, s, NH); 7.60 (1H, s, H triazole); 7.24–7.17 (4H, m, H Ar); 6.26 (1H, s, CH); 5.22 (2H, dd, $J = 15.2$, $J = 15.1$, CH₂); 4.91 (1H, d, $J = 16.2$, CH₂ pyrazine); 3.98 (1H, d, $J = 16.2$, CH₂ pyrazine); 2.31 (3H, s, CH₃); 1.27 (9H, s, C(CH₃)₃). ¹³C NMR spectrum, δ , ppm: 168.8; 163.5; 138.1; 132.4; 129.8; 129.5; 129.4 (2C); 129.3; 59.2; 51.0; 49.2; 28.9; 21.2; 5.2. Found, %: C 63.25; H 6.74; N 20.45. C₁₈H₂₃N₅O₂. Calculated, %: C 63.32; H 6.79; N 20.51.

2-(4-Chlorophenyl)-*N*-cyclohexyl-2-(6-oxo-6,7-dihydro-[1,2,3]triazolo[1,5-*a*]pyrazin-5(4*H*)-yl)acetamide (3c). Yield 0.368 g (95%), white solid, mp 215–217°C. IR spectrum, ν , cm⁻¹: 3118, 1669, 1623, 1441, 1062. ¹H NMR spectrum, δ , ppm (J , Hz): 8.35 (1H, d, $J = 7.8$, NH); 7.61 (1H, s, H triazole); 7.50 (2H, d, $J = 8.0$, H Ar); 7.31 (2H, d, $J = 8.2$, H Ar); 6.30 (1H, s, CH); 5.22 (2H, dd, $J = 17.7$, $J = 17.3$, CH₂); 4.93 (1H, d, $J = 16.1$, CH₂ pyrazine); 4.11 (1H, d, $J = 16.1$, CH₂ pyrazine); 3.63–3.61 (1H, m, CH cyclohexyl); 1.80–1.53 (5H, m, CH₂ cyclohexyl); 1.30–1.06 (5H, m, CH₂ cyclohexyl). ¹³C NMR spectrum, δ , ppm: 167.6; 163.7; 134.2; 133.5; 131.3; 129.5; 129.4; 129.3; 58.6; 49.3; 48.3; 32.6; 25.6; 25.0; 24.9. Found, %: C 58.78; H 5.65; N 18.09. C₁₉H₂₂ClN₅O₂. Calculated, %: C 58.84; H 5.72; N 18.06.

***N*-Cyclohexyl-2-(4-methylphenyl)-2-(6-oxo-6,7-dihydro-[1,2,3]triazolo[1,5-*a*]pyrazin-5(4*H*)-yl)acetamide (3d).** Yield 0.345 g (94%), white solid, mp 163–165°C. IR spectrum, ν , cm⁻¹: 3119, 1664, 1628, 1439, 1071. ¹H NMR spectrum, δ , ppm (J , Hz): 8.49 (1H, d, $J = 10.0$, NH); 7.79 (1H, s, H triazole); 7.42 (2H, d, $J = 8.0$, H Ar); 7.37 (2H, d, $J = 8.0$, H Ar); 6.47 (1H, s, CH); 5.20 (2H, dd, $J = 17.6$, $J = 17.5$, CH₂); 5.12 (1H, d, $J = 15.0$, CH₂ pyrazine); 4.24 (1H, d, $J = 16.1$, CH₂ pyrazine); 3.81–3.79 (1H, m, CH cyclohexyl); 3.55 (3H, s, CH₃); 1.94–1.71 (5H, m, CH₂ cyclohexyl); 1.43–1.28 (5H, m, CH₂ cyclohexyl). ¹³C NMR spectrum, δ , ppm: 168.1; 163.6; 138.2; 132.1; 129.9; 129.4; 129.3; 59.0 (2C); 49.2; 48.3; 32.7; 32.6; 25.6; 25.0; 24.9; 21.1. Found, %: C 65.43; H 6.90; N 18.99. C₂₀H₂₅N₅O₂. Calculated, %: C 65.37; H 6.86; N 19.06.

***N*-tert-Butyl-2-(4-chlorophenyl)-2-(6-oxo-6,7-dihydro-[1,2,3]triazolo[1,5-*a*]pyrazin-5(4*H*)-yl)acetamide (3e).** Yield 0.347 g (96%), white solid, mp 221–223°C. IR spectrum, ν , cm⁻¹: 3126, 1665, 1619, 1442, 1069. ¹H NMR spectrum, δ , ppm (J , Hz): 8.14 (1H, s, NH); 7.61 (1H, s, H triazole); 7.51 (2H, d, $J = 8.2$, H Ar); 7.29 (2H, d, $J = 8.1$, H Ar); 6.29 (1H, s, CH); 5.23 (2H, dd, $J = 17.5$, $J = 17.3$, CH₂); 4.93 (1H, d, $J = 16.0$, CH₂ pyrazine); 4.03 (1H, d, $J = 16.2$, CH₂ pyrazine); 1.27 (9H, s, C(CH₃)₃). ¹³C NMR spectrum, δ , ppm: 168.3; 163.7; 134.5; 133.5; 131.3; 129.5; 129.4; 129.3; 58.7; 58.6; 51.2; 49.3; 28.8. Found, %: C 56.47; H 5.63; N 19.27. C₁₇H₂₀ClN₅O₂. Calculated, %: C 56.43; H 5.57; N 19.36.

***N*-Cyclohexyl-2-(3-methylphenyl)-2-(6-oxo-6,7-dihydro-[1,2,3]triazolo[1,5-*a*]pyrazin-5(4*H*)-yl)acetamide (3f).** Yield 0.349 g (95%), white solid, mp >250°C. IR spectrum, ν , cm⁻¹: 3121, 1659, 1625, 1432, 1058. ¹H NMR spectrum, δ , ppm (J , Hz): 8.31 (1H, d, $J = 8.0$, NH); 7.61 (1H, s, H triazole); 7.30 (1H, t, $J = 7.4$, H Ar); 7.19 (1H, d, $J = 7.3$, H Ar); 7.08–7.06 (2H, m, H Ar); 6.27 (1H, s, CH); 5.20 (2H, dd, $J = 18.5$, $J = 18.4$, CH₂); 4.93 (1H, d, $J = 16.3$, CH₂ pyrazine); 4.05 (1H, d, $J = 16.9$, CH₂ pyrazine); 3.62 (1H, br. s, CH cyclohexyl); 2.31 (3H, s, CH₃); 1.79–1.52 (5H, m, CH₂ cyclohexyl); 1.27–1.11 (5H, m, CH₂ cyclohexyl). ¹³C NMR spectrum, δ , ppm: 167.6; 163.1; 138.0; 134.6; 129.5; 129.0 (2C); 128.7; 125.9; 58.7; 48.8; 47.8; 32.2; 25.1; 24.5; 24.4; 21.0. Found, %: C 65.43; H 6.80; N 19.03. C₂₀H₂₅N₅O₂. Calculated, %: C 65.37; H 6.86; N 19.06.

***N*-tert-Butyl-2-(4-methoxyphenyl)-2-(6-oxo-6,7-dihydro-[1,2,3]triazolo[1,5-*a*]pyrazin-5(4*H*)-yl)acetamide (3g).** Yield 0.343 g (96%), white solid, mp 192–194°C. IR spectrum, ν , cm⁻¹: 3118, 1667, 1621, 1438, 1066. ¹H NMR spectrum, δ , ppm (J , Hz): 8.03 (1H, s, NH); 7.60 (1H, s, H triazole); 7.22 (2H, d, $J = 8.3$, H Ar); 6.99 (2H, d, $J = 8.3$, H Ar); 6.25 (1H, s, CH); 5.21 (2H, dd, $J = 17.5$, $J = 17.2$, CH₂); 4.92 (1H, d, $J = 16.0$, CH₂ pyrazine); 4.00 (1H, d, $J = 16.2$, CH₂ pyrazine); 3.77 (3H, s, OCH₃); 1.28 (9H, s, C(CH₃)₃). ¹³C NMR spectrum, δ , ppm: 169.0; 163.5; 159.6; 130.8; 129.5; 129.5; 127.1; 114.7; 58.9 (2C); 55.6; 51.0; 49.2; 40.0; 28.9. Found, %: C 60.43; H 6.46; N 19.65. C₁₈H₂₃N₅O₃. Calculated, %: C 60.49; H 6.49; N 19.59.

***N*-tert-Butyl-2-(6-oxo-6,7-dihydro-4*H*-[1,2,3]triazolo[1,5-*a*]pyrazin-5-yl)-2-(3,4,5-trimethoxyphenyl)acetamide (3h).** Yield 384 g (92%), white solid, mp 190–192°C. IR spectrum, ν , cm⁻¹: 3115, 1670, 1621, 1437, 1060. ¹H NMR spectrum, δ , ppm (J , Hz): 8.10 (1H, s, NH); 7.62 (1H, s, H triazole); 6.54 (1H, s, H Ar); 6.21 (1H, s, CH); 5.22 (2H, dd, $J = 17.5$, $J = 17.3$, CH₂); 4.93 (1H, d, $J = 16.3$, CH₂ pyrazine); 4.08 (1H, d, $J = 16.3$, CH₂ pyrazine); 3.74 (6H, s, 2OCH₃); 3.68 (3H, s, OCH₃); 1.29 (9H, s, C(CH₃)₃). ¹³C NMR spectrum, δ , ppm: 168.7; 163.5; 153.4; 137.8; 130.8; 129.7; 129.5; 106.7; 60.5; 59.5; 56.3 (2C); 51.1; 49.2; 28.8. Found, %: C 57.58; H 6.58; N 16.81. C₂₀H₂₇N₅O₅. Calculated, %: C 57.54; H 6.52; N 16.78.

***N*-Cyclohexyl-2-(4-isopropylphenyl)-2-(6-oxo-6,7-dihydro-[1,2,3]triazolo[1,5-*a*]pyrazin-5(4*H*)-yl)acetamide (3i).** Yield 0.371 g (94%), white solid, mp 192–194°C. IR spectrum, ν , cm⁻¹: 3118, 1670, 1629, 1429, 1057. ¹H NMR spectrum, δ , ppm (J , Hz): 8.30 (1H, s, NH); 7.61 (1H, s, H triazole); 7.29–7.21 (4H, m, H Ar); 6.29 (1H, s, CH); 5.29–5.13 (2H, m, CH₂); 4.95 (1H, d, $J = 16.0$, CH₂ pyrazine); 4.05 (1H, d, $J = 16.4$, CH₂ pyrazine); 3.63 (1H, br. s, CH cyclohexyl); 3.22 (1H, s, CH); 2.95–2.83 (1H, m, CH(CH₃)₂); 1.81–1.53 (5H, m, CH₂ cyclohexyl); 1.24–1.13 (11H, m, CH₂ cyclohexyl, CH(CH₃)₂). ¹³C NMR spectrum, δ , ppm: 168.1; 163.6; 149.0; 132.6; 129.5; 129.4; 127.2; 126.4; 58.9; 53.0; 49.2; 48.3; 33.6; 32.7; 25.6; 25.0 (2C); 24.3. Found, %: C 68.87; H 7.40; N 17.75. C₂₂H₂₉N₅O₂. Calculated, %: C 66.81; H 7.39; N 17.71.

***N*-tert-Butyl-2-(4-isopropylphenyl)-2-(6-oxo-6,7-dihydro-4*H*-[1,2,3]triazolo[1,5-*a*]pyrazin-5-yl)acetamide (3j).** Yield 0.354 g (96%), white solid, mp 188–190°C. IR spectrum, ν , cm⁻¹: 3119, 1662, 1616, 1431, 1064. ¹H NMR spectrum, δ , ppm (J , Hz): 8.08 (1H, s, NH); 7.61 (1H, s, H triazole); 7.31 (2H, d, $J = 8.1$, H Ar); 7.22 (2H, d, $J = 8.1$, H Ar);

6.30 (1H, s, CH); 5.23 (2H, dd, $J = 17.4$, $J = 17.4$, CH₂); 4.96 (1H, d, $J = 16.2$, CH₂ pyrazine); 4.00 (1H, d, $J = 16.1$, CH₂ pyrazine); 2.90 (1H, septet, $J = 13.6$, CH(CH₃)₂); 1.29 (9H, s, C(CH₃)₃); 1.21 (6H, d, $J = 8.7$, CH(CH₃)₂). ¹³C NMR spectrum, δ , ppm: 168.8; 163.5; 148.9; 132.9; 129.5 (2C); 129.3; 127.2; 59.0; 51.1; 49.2; 33.6; 28.9; 24.3; 24.2. Found, %: C 65.07; H 7.29; N 18.93. C₂₀H₂₇N₃O₂. Calculated, %: C 65.02; H 7.37; N 18.96.

Evaluation of *in vitro* antibacterial activity. The minimum inhibitory concentration (MIC) of all samples was evaluated by microdilution method according to the guidelines presented by Clinical and Laboratory Standards Institute.²⁷ To achieve this purpose, a serial dilution of each sample was performed in a 96-well microplate using Mueller–Hinton Broth (MHB) medium. Two Gram-negative bacteria *Staphylococcus aureus* (ATCC 29737), *Enterococcus faecalis* (ATCC 29212) and two Gram-positive bacteria *Escherichia coli* (ATCC 25922) and *Pseudomonas aeruginosa* (ATCC 27853) were used in this study. The microorganisms were cultured in Brain Heart Infusion (BHI) broth overnight and then were applied for antimicrobial testing. For this, each microbial strain was cultured in MHB to match the turbidity of 1.5×10^8 CFU/ml. To prepare bacterial suspensions for inoculation, this suspension was diluted to yield 5×10^6 CFU/ml. Finally, 10 μ l of the prepared suspension was inoculated into each microplate well. After an overnight incubation at 37°C, the optical density of the wells was obtained by an ELISA reader apparatus (BioTek, Power Wave XS2) at wavelength 600 nm. In this assay, ampicillin and culture media served as positive and negative controls, respectively. The MIC was defined as lowest concentration of antimicrobial agents that inhibited 90% of the bacterial growth after an overnight incubation in comparison with negative control.

Supplementary information file containing ¹H and ¹³C NMR spectra of all synthesized compounds is available at the journal website at <http://link.springer.com/journal/10593>.

References

- Deak, D.; Outtersson, K.; Powers, J. H.; Kesselheim, A. S. *Ann. Int. Med.* **2016**, *165*, 363.
- (a) Wu, Y.; Ding, X.; Ding, L.; Zhang, Y.; Cui, L.; Sun, L.; Li, W.; Wang, D.; Zhao, Y. *Eur. J. Med. Chem.* **2018**, *158*, 247. (b) Sunny, T. P.; Jacob, R.; Krishnakumar, K.; Varghese, S. *Nat. J. Physiol. Pharm. Pharmacol.* **2019**, *9*, 821.
- Su, L.; Li, J.; Zhou, Z.; Huang, D.; Zhang, Y.; Pei, H.; Guo, W.; Wu, H.; Wang, X.; Liu, M.; Yang, C.-G.; Chen, Y. *Eur. J. Med. Chem.* **2019**, *162*, 203.
- Hu, Y.-Q.; Zhang, S.; Xu, Z.; Lv, Z.-S.; Liu, M.-L.; Feng, L.-S. *Eur. J. Med. Chem.* **2017**, *141*, 335.
- Kant, R.; Singh, V.; Nath, G.; Awasthi, S. K.; Agarwal, A. *Eur. J. Med. Chem.* **2016**, *124*, 218.
- Kolb, H. C.; Sharpless, K. B. *Drug Discovery Today* **2003**, *8*, 1128.
- Joshi, S.; More, U. A.; Kulkarni, V. H. *Indian J. Pharm. Sci.* **2013**, *75*, 310.
- Huo, X.-Y.; Guo, L.; Chen, X.-F.; Zhou, Y.-T.; Zhang, J.; Han, X.-Q.; Dai, B. *Molecules* **2018**, *23*, 1344.
- Abbaspour, S.; Keivanloo, A.; Bakherad, M.; Sepehri, S. *Chem. Biodiversity* **2018**, *16*, e1800410.
- Shaikh, M. H.; Subhedar, D. D.; Nawale, L.; Sarkar, D.; Khan, F. A. K.; Sangshetti, J. N.; Shingate, B. B. *MedChemComm* **2015**, *6*, 1104.
- Ma, L.-Y.; Pang, L.-P.; Wang, B.; Zhang, M.; Hu, B.; Xue, D.-Q.; Shao, K.-P.; Zhang, B.-L.; Liu, Y.; Zhang, E.; Liu, H.-M. *Eur. J. Med. Chem.* **2014**, *86*, 368.
- Khanetsky, B.; Dallinger, D.; Kappe, C. O. *J. Comb. Chem.* **2004**, *6*, 884.
- Hassan, H. M. A.; Denetiu, I.; Sakkaf, K.; Khan, K. A.; Pushparaj, P. N.; Gauthaman, K. *Heterocycles* **2017**, *94*, 1856.
- (a) Whiting, M.; Muldoon, J.; Lin, Y. C.; Silverman, S. M.; Lindstrom, W.; Olson, A. J.; Kolb, H. C.; Finn, M. G.; Sharpless, K. B.; Elder, J. H. *Angew. Chem., Int. Ed.* **2006**, *45*, 1435. (b) Thirumurugan, P.; Matusiuk, D.; Jozwiak, K. *Chem. Rev.* **2013**, *113*, 4905. (c) Manetsch, R.; Krasinski, A.; Radić, Z.; Raushel, J.; Taylor, P.; Sharpless, K. B.; Kolb, H. C. *J. Am. Chem. Soc.* **2004**, *126*, 12809.
- Bonyasi, R.; Gholinejad, M.; Saadati, F.; Nájera, C. *New J. Chem.* **2018**, *42*, 3078.
- Saadati, F.; Gholinejad, M.; Janmohammadi, H.; Shaybanizadeh, S. *Lett. Org. Chem.* **2018**, *15*, 79.
- (a) Beletskaya, I. P.; Cheprakov, A. V. *Coord. Chem. Rev.* **2004**, *248*, 2337. (b) Ley, S. V.; Thomas, A. W. *Angew. Chem., Int. Ed.* **2003**, *42*, 5400.
- (a) Bahadorikhalili, S.; Ma'mani, L.; Mahdavi, H.; Shafiee, A. *Microporous Mesoporous Mater.* **2018**, *262*, 207. (b) Mahdavi, M.; Lijan, H.; Bahadorikhalili, S.; Ma'mani, L.; Ranjbar, P. R.; Shafiee, A. *RSC Adv.* **2016**, *6*, 28838. (c) Sayahi, M. H.; Bahadorikhalili, S.; Saghanezhad, S. J.; Mahdavi, M. *Res. Chem. Intermed.* **2018**, *44*, 5241. (d) Sayahi, M. H.; Saghanezhad, S. J.; Bahadorikhalili, S.; Mahdavi, M. *Appl. Organomet. Chem.* **2019**, *33*, e4635. (e) Biradar, A. V.; Biradar, A. A.; Asefa, T. *Langmuir* **2011**, *27*, 14408. (f) Nasr-Esfahani, M.; Mohammadpoor-Baltork, I.; Khosropour, A. R.; Moghadam, M.; Mirkhani, V.; Tangestaninejad, S. *J. Mol. Catal. A: Chem.* **2013**, *379*, 243.
- Bahadorikhalili, S.; Ashtari, A.; Ma'mani, L.; Ranjbar, P. R.; Mahdavi, M. *Appl. Organomet. Chem.* **2018**, *32*, e4212.
- (a) Song, X.; She, Y.; Ji, H.; Zhang, Y. *Org. Process Res. Dev.* **2005**, *9*, 297. (b) Zhao, X.; Kong, A.; Shan, C.; Wang, P.; Zhang, X.; Shan, Y. *Catal. Lett.* **2009**, *131*, 526.
- (a) Cruz, P.; Pérez, Y.; del Hierro, I.; Fajardo, M. *Microporous Mesoporous Mater.* **2016**, *220*, 136. (b) Tang, Q.; Gong, X.; Zhao, P.; Chen, Y.; Yang, Y. *Appl. Catal., A* **2010**, *389*, 101.
- (a) Zhao, H.; Chen, Q.; Wei, L.; Jiang, Y.; Cai, M. *Tetrahedron* **2015**, *71*, 8725. (b) Hamza, A.; Srinivas, D. *Catal. Lett.* **2009**, *128*, 434. (c) Lv, W.; Tian, J.; Deng, N.; Wang, Y.; Zhu, X.; Yao, X. *Tetrahedron Lett.* **2015**, *56*, 1312.
- (a) Rostovtsev, V. V.; Green, L. G.; Fokin, V. V.; Sharpless, K. B. *Angew. Chem.* **2002**, *114*, 2708. (b) Nasr-Esfahani, M.; Mohammadpoor-Baltork, I.; Khosropour, A. R.; Moghadam, M.; Mirkhani, V.; Tangestaninejad, S.; Amiri Rudbari, H. *J. Org. Chem.* **2014**, *79*, 1437.
- (a) Sonogashira, K. *J. Organomet. Chem.* **2002**, *653*, 46. (b) Hamza, A.; Tréguier, B.; Brion, J.-D.; Alami, M. *Org. Biomol. Chem.* **2011**, *9*, 6200.
- (a) Gholinejad, M.; Afrasi, M.; Nikfarjam, N.; Nájera, C. *Appl. Catal., A* **2018**, *563*, 185. (b) Gholinejad, M.; Zareh, F.; Nájera, C. *Appl. Organomet. Chem.* **2018**, *32*, e3984. (c) Schätz, A.; Grass, R. N.; Stark, W. J.; Reiser, O. *Chem.–Eur. J.* **2008**, *14*, 8262. (d) Yarie, M.; Zolfigol, M. A.; Bayat, Y.; Asgari, A.; Alonso, D. A.; Khoshnood, A. *RSC Adv.* **2016**, *6*, 82842. (e) Moradi, S.; Zolfigol, M. A.; Zarei, M.; Alonso, D. A.; Khoshnood, A.; Tajally, A. *Appl. Organomet. Chem.* **2018**, *32*, e4043.
- Zhu, Y.; Stubbs, L. P.; Ho, F.; Liu, R.; Ship, C. P.; Maguire, J. A.; Hosmane, N. S. *ChemCatChem* **2010**, *2*, 365.
- Lee, S. M.; Kim, J.; Jeong, J.; Park, Y. K.; Bai, G.-H.; Lee, E. Y.; Lee, M. K.; Chang, C.L. *J. Korean Med. Sci.* **2007**, *22*, 784.